In vitro cytocompatibility evaluation of poly(octamethylene citrate) monomers toward their use in orthopedic regenerative engineering

Chuying Ma [a], Ethan Gerhard [a], Qiaoling Lin [a], Silun Xia [b], April Dawn Armstrong [c], Jian Yang [a], *

[a] Department of Biomedical Engineering, Materials Research Institute, The Huck Institutes of the Life Sciences, The Pennsylvania State University, University Park, PA 16802, USA
[b] CATS College, Canterbury, Kent CT1 3LQ, UK
[c] Department of Orthopaedics and Rehabilitation, College of Medicine, The Pennsylvania State University, Hershey, PA 17033, USA

ABSTRACT

Citrate based polymer poly(octamethylene citrate) (POC) has shown promise when formulated into composite material containing up to 65 wt% hydroxylapatite (HA) for orthopedic applications. Despite significant research into POC, insufficient information about the biocompatibility of the monomers 1,8-Octanediol and Citrate used in its synthesis is available. Herein, we investigated the acute cytotoxicity, immune response, and long-term functionality of both monomers. Our results showed a cell-type dependent cytotoxicity of the two monomers: 1,8-Octanediol induced less acute toxicity to 3T3 fibroblasts than Citrate while presenting comparable cytotoxicity to MG63 osteoblast-like cells; however, Citrate demonstrated enhanced compatibility with hMSCs compared to 1,8-Octanediol. The critical cytotoxic concentration values EC30 and EC50, standard for comparing cytotoxicity of chemicals, were also provided. Additionally, Citrate showed slower and less inhibitory effects on long-term hMSC cell proliferation compared with 1,8-Octanediol. Furthermore, osteogenic differentiation of hMSCs exposure to Citrate resulted in less inhibitory effect on alkaline phosphatase (ALP) production. Neither monomer triggered undesired pro-inflammatory responses. In combination with diffusion model analysis of monomer release from cylindrical implants, based on which the maximum concentration of monomers in contact with bone tissue was estimated to be 2.2×10^{-4} mmol/L, far lower than the critical cytotoxic concentrations as well as the 1,8-Octanediol concentration (0.4 mg/mL or 2.7 mmol/L) affecting hMSCs differentiation, we provide strong evidence for the cytocompatibility of the two monomers degraded from citrate-based composites in the orthopedic setting.

© 2018 The Authors. Production and hosting by Elsevier B.V. on behalf of KeAi Communications Co., Ltd. This is an open access article under the CC BY-NC-ND license (http://creativecommons.org/licenses/by-nc-nd/4.0/).

1. Introduction

Despite the innate regenerative capacity of human bone, healing of nonunion defects, defined as incomplete defect closure, remains a challenge clinically, creating a substantial need for the development of bone grafts to bridge defects and guide tissue regeneration [1]. The development of orthopedic biomaterials that are totally synthetic, readily available, capable of fully degrading in vivo, and mimic natural bone has been strongly encouraged to replace the limited supply of autografts [2–4]. Notably, citrate based materials with rich -COOH groups capable of incorporating up to 65 wt% of hydroxylapatite (HA), simulating the inorganic composition of natural bone, have shown great promise in bone regeneration compared to traditional degradable polymers such as polylactide (PLA) capable of compositing a maximum of 25–30 wt% of HA before becoming excessively brittle [5]. In contrast to PLA's bulk degradation, the degradation of citrate-based material proceeds in a form of surface erosion, which could avoid the accumulation of massive acidic degradation products [6]. Moreover, the strongest citrate based polymer/HA composites possessed a compressive strength of ~250 MPa, falling within the range of human cortical bone (100–230 MPa) [7]. Therefore, citrate-based polymers could serve as ideal base materials to prepare bone-like composite

orthopedic biomaterials [7,8].

The first citrate-based polymer composited with HA for orthopedic applications was poly(octamethylene citrate) (POC) synthesized by reacting Citric Acid and 1,8-Octanediol through a convenient one-pot polycondensation reaction [5,8–10]. In addition to POC, both Citrate and 1,8-Octanediol have been widely used for the synthesis of a family of citrate-derived polymers with various functionalities for diversified applications such as soft and hard tissue engineering, drug delivery, bioimaging, and biosensing in the last decade [5,11–21]. Although both *in vitro* and *in vivo* biocompatibility of POC and POC/HA composites have been well tested in previous studies [5,8,10], there is surprisingly limited information about the safety of the two monomers given the cytocompatibility of individual components of materials should be considered at the onset of materials design [22–24]. Moreover, *in vivo* degradability of POC/HA is a highly desired material property that allows gradual replacement of the bulk implant with functional tissue. The main degradation mechanism is cleavage of the ester bond formed by Citrate and 1,8-Octanediol [5]. It means that Citrate and 1,8-Octanediol would comprise the majority of the degradation products of POC/HA, and would readily contact with host tissue, largely affecting the long-term tissue response. Citrate has historically been regarded as a biocompatible monomer, since it is a well-known naturally occurring metabolite in the TCA cycle, and its application in certain medical situations has been approved by the FDA: for example, the citrate containing drug "PREPOPIK" has been approved for cleansing of the colon as a preparation for colonoscopy. However, almost no biocompatibility information is available for its orthopedic applications. In comparison, the safety of 1,8-Octanediol in biomedical applications remains much more underexplored, although 1,8-Octandiol has been reported to be used in cosmetics as a plasticizer [25].

In the present study, we filled the blanks by investigating the biocompatibility of the two POC monomers to different cells with the objective of answering the following questions: 1) Is toxicity of Citrate or 1,8-Octanediol cell-type dependent? 2) What are the tolerant concentrations of the two monomers to different cells? 3) What are the critical concentrations of the two monomers for bone forming cells to maintain their functionality towards bone formation? 4) How do we estimate the *in vivo* release and diffusion of monomers from implants, particularly from cylindrical implants often tested in animal studies, after material degradation? Answering the above questions is critical for the future translation of the biomaterials made of Citrate and 1,8-Octanediol.

2. Material and methods

2.1. Solution preparation

1,8-Octanediol (Alfa Aesar), which is sparingly soluble in water, was dissolved using complete medium to prepare fresh solutions at the concentration of 15 mg/mL and was subjected to further dilution using complete medium prior to testing. Citrate (Alfa Aesar) stock solution at the concentration of 150 mg/mL was prepared with DI water and buffered to pH 7.2–7.4 with 1N NaOH solution, followed by aliquoting and storage at −20 °C. Sodium dodecylsulfate salt (SDS) stock solution was prepared with DI water at a concentration of 2 mg/mL followed by aliquoting and storage at −20 °C.

2.2. Cell culture

Mouse fibroblast cells 3T3 and human osteoblast-like cells MG63 were purchased from ATCC and maintained in high glucose Dulbecco's Modified Eagle Medium (DMEM; Sigma) supplemented with 10% fetal bovine serum (FBS). Human mesenchymal stem cells (hMSCs) were obtained from Lonza and cultured with low glucose DMEM with 10% FBS and GlutaMAX (Gibico). hMSCs with passage ≤7 were used in the present study. All the cells were cultured in a humidified atmosphere with 5% CO_2 at 37 °C. Human acute monocytic leukemia cells THP-1 obtained from ATCC were cultured in suspension using RPMI-1640 with 20% FBS and 0.05 mM 2-Mercaptoethanol, with the culture flask placed upright for better cell recovery. After passage cells one time, the culture flask was lied down and cells were maintained in complete RPMI-1640 medium with 10% FBS and 0.05 mM 2-Mercaptoethanol.

2.3. Cytotoxicity evaluation

All *in vitro* cytotoxicity tests were conducted according to the international standard ISO 10993-5:2009(E). Dilutions of SDS producing a reproducible cytotoxic response served as positive control while blank wells without the test sample served as negative control to reflect the background response. Both positive and negative controls were included in each assay. Briefly, cells were seeded to 96 well plates at desired density (Seeding density: 3T3, 20,000 cells/cm^2; MG63, 20,000 cells/cm^2; hMSCs, 10,000 cells/cm^2). After the cultured cells reached subconfluency (approximately 80% confluency), the culture medium was removed and 100 μL of 1,8-Octanediol, Citrate or SDS solution at various concentrations were added to cells. After incubation for 24 h, the medium was removed followed by the addition of Cell Counting Kit-8 (CCK-8; Dojindo) solution diluted 1:10 with complete medium. Finally, the absorbance was measured at 450 nm with a Microplate reader.

2.4. Cell proliferation assay

In the cell proliferation assay, hMSCs were seeded to 96 well plates at a density of 5000 cells/cm^2. After 24 h, culture medium was removed and test samples at different concentrations were added and cultured with cells for 1, 3, and 5 days. Finally, CCK-8 assay was performed according to manufacture instructions. Proliferation rate was identified as the increasing in cell viability/day from day 1-day 3 and day 3-day 5, respectively.

2.5. Osteogenic differentiation of hMSCs

To test the effect on osteogenic differentiation, hMSCs at passage≤7 were used. Cells were seeded to 48 well plates at a density of 10,000 cells/cm^2, and cultured to reach subconfluency. Then, differentiation was initiated by adding osteogenic medium supplemented with 10^{-7} M Dexamethasome, 0.05 mM ascorbate-2-phosphate, and 0.01M β-glycerophosphate. Dilutions of 1,8-Octanediol and Citrate were added in osteogenic medium to test their effect on differentiation.

2.6. ALP assay and ALP staining

After differentiation for 14 days, part of the cell sample was collected for alkaline phosphatase (ALP) assay while the other part was fixed for ALP staining. In the ALP assay, cells were first washed twice with PBS and lysed with RIPA lysis buffer. Then, the cell lysate was transferred to microcentrifuge tubes and centrifuged at 14,000 g for 15 min at 4 °C. The supernatant was subsequently transferred to a new tube and a PicoGreen DNA quantification assay (Molecular Probes) was performed to determine total DNA concentration in lysate according to the manufacturer's instructions. Meanwhile, the cell lysate was diluted with Assay buffer to a final volume of 50 μL per sample and added to 96 well plates. Stock

solution of ALP substrate p-Nitrophenyl Phosphate (pNPP; 1M; Sigma) was diluted 1:100 with cold ALP Assay buffer to prepare the pNPP working solution, 50 μL of which was added to 96 well plates and incubated with cell lysate for 10−40 min at 37 °C. The reaction was finally stopped by adding 50 μL of 0.9 M NaOH as stopping solution to each well, and the absorbance at 405 nm was measured on a Microplate reader. For ALP staining, a Leukocyte Alkaline Phosphatase kit (Sigma-Aldrich) based on Naphthol AS-MX phosphate and Fast blue RR salt was used to stain the ALP activity in fixed cells according to manufacturer's instructions.

2.7. Measurement of TNF-α and IL-1β release

THP-1 cells were collected by centrifuging at 1500 rpm for 5 min and resuspended with complete medium. After cell counting, 700 μL of diluted cell suspension at a density of 10^6 cells/mL with/without test samples was added to 48 well plates. 50 ng of Lipopolysaccharides (LPS) from Escherichia coli0111:B4 (Sigma) that positively activate THP-1 to produce inflammatory factors was added to THP-1 cell suspensions as a positive control. After cultured for 18 h [26] in a humidified atmosphere with 5% CO_2 at 37 °C, cell suspensions in each group were transferred to 1.5 mL centrifuge tubes and centrifuged at 1500 rpm for 5 min. Supernatant was collected and transferred to a new tube, while the cell pellet was resuspended with 100 μL CCK-8 assay solution diluted 1:10 with complete medium, and the cell viability was measured using a Microplate reader at 450 nm after 30 min of incubation. The supernatant samples were subjected to ELISA tests (R&D systems) for the determination of TNF-α and IL-1β released by THP-1 cells according to manufacturer's instructions.

2.8. Statistic analysis

Each data point represents an average of 5 (Cytotoxicity evaluation; Cell proliferation assay) or 4 samples (ALP assay; ELISA assay), with at least 2 replicates of each experiment. Ordinary One-way ANOVA was performed using standard methods for the Tukey multiple comparison test. P < 0.05 was regarded as significant.

2.9. Chemical diffusion model for degradable implants

To evaluate the biocompatibility and efficacy of POC/HA in vivo, cylindrical implants were often tested in animal models. For a POC/60%HA implant with a radius (R) of 1.35 mm and height (L) of 4 mm, density (ρ) is 6.13 g cm^{-3}, and constituent monomers Citrate and 1,8-Octanediol (1:1 mol ratio) could be released from the implant in a zero order manner for 1 year [8]. As shown in Fig. 1, assuming
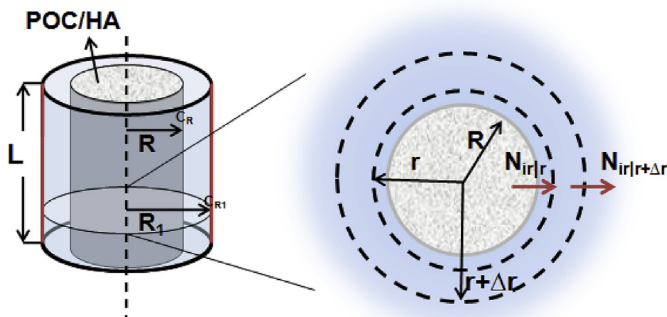

Fig. 1. Radial diffusion through a cylindrical area.

bone is homogenous, and the transport is only in the radial direction without any chemical reaction, then after cylindrical POC/HA is implanted, there is a concentration gradient of released monomers between our implant surface (r = R = 1.35 mm) with high concentration of monomer set to C_R and the blood vessel rich surface (r = R_1 = 1.55 mm) where the monomer concentration C_{R1} is 0 given the time for the monomers to flux into the blood stream through vessel walls compared with the time to diffuse toward the blood vessels is short enough and all cells have to be within 200 μm from a blood vessel [27]. Between the two surfaces is the control volume defined as the bone tissue volume that could be affected by the released monomers. Based on the above assumptions, the concentration profile, flux of monomers out of the defined bone tissue volume, and the maximum concentration at implant surface C_R can be determined as follows:

Part 1: Based on the radial diffusion model in cylindrical co-ordinates [28], the following equation based on mass balance through a volume element $2\pi rL\Delta r$ without chemical reactions can be generated:

$$\frac{\partial C_i}{\partial t}2\pi rL\Delta r = \left(N_{ir/r}(r) - N_{ir/(r+\Delta r)}(r + \Delta r)\right)2\pi L \quad (1.1)$$

where C_i is the molar concentration of component i, and N_i is the molar flux (the amount of component i crossing a unit area per unit time). Then dividing each term of the equation by the volume element $2\pi rL\Delta r$ leads to the formula:

$$\frac{\partial C_i}{\partial t} = \frac{\left(N_{ir/r}(r) - N_{ir/(r+\Delta r)}(r + \Delta r)\right)}{r\Delta r} \quad (1.2)$$

Taking the limit as $\Delta r \to 0$ gives the following differential expression based on the basic definition of the derivative:

$$\frac{\partial C_i}{\partial t} = -\frac{1}{r}\frac{\partial(rN_{ir})}{\partial r} \quad (1.3)$$

Applying Fick's Law for diffusion without convection $\left(N_{ir} = -D_{ij}\frac{\partial C_i}{\partial r}\right)$ into Eq. (1.3) results in:

$$\frac{\partial C_i}{\partial t} = \frac{D_{ij}}{r}\frac{\partial}{\partial r}\left(r\frac{\partial C_i}{\partial r}\right)_i \quad (1.4)$$

where D_{ij} is the diffusion coefficient of component i in solvent j. Considering one-dimensional radial diffusion at steady state, meaning $\frac{\partial C_i}{\partial t} = 0$, then the above equation can be reduced to be:

$$\frac{1}{r}\frac{d}{dr}\left(r\frac{dC_i}{dr}\right) = 0 \quad (1.5)$$

Integrate Eq. (1.5) twice to get:

$$C_i = A \ln r + B \quad (1.6)$$

Applying the boundary conditions r = R (1.35 mm), $C_i = C_R$ and r = R_1 (1.55 mm), $C_i = 0$, yields:

$$A = \frac{C_R}{\ln 1.35 - \ln 1.55} = \frac{C_R}{-0.14} \quad B = \frac{C_R \times \ln 1.55}{\ln 1.55 - \ln 1.35} = 3.14C_R$$

Thus, the concentration profile is:

$$C = \frac{C_R}{-0.14}\ln r + 3.14C_R \quad (1.7)$$

Applying the diffusion coefficient value D of fluorescein (0.0198 mm^2 min^{-1}) in mice cortical bone published previously

[29], the molar flux out of the bone tissue volume is:

$$N_i = -D_{ij}\frac{dC_i}{dr} = D_{ij}\frac{C_R}{0.14r} = 0.14\frac{C_R}{r} \tag{1.8}$$

So the Flux at r = R_1 is:

$$N = 0.09C_R \left(\text{mol cm}^{-2}\text{s}^{-1}\right) \tag{1.9}$$

Part 2:Based on the known size and density of the POC/60%HA implant, its mass m is:

$$m = \rho\pi R^2 L = 0.14\text{ g} = 140\text{ mg} \tag{2.1}$$

The POC weight as well as the Citrate and 1,8-Octanediol amount can be determined, since 40 wt% POC was composited with 60 wt% Hydroxylapatite, and Citrate and 1,8-Octanediol were synthesized at 1:1 mol ratio:

$$m_{POC} = 56\text{ mg}$$

$$M_{\text{Citrate}} = \frac{31.8(mg)}{192(g/mol)} = 0.165\text{ (mmol)} \quad M_{\text{Octanediol}} = \frac{24.2(mg)}{146(g/mol)}$$
$$= 0.165\text{ (mmol)}$$

where M_i is the molar mass of component i. Assuming the implant could fully degrade in 1 year, then molar flux into bone tissue volume is

$$N = \frac{M}{2\pi RLt} \tag{2.2}$$

Applying known parameters into Eq. (2.2), we are able to get

$$N_{\text{Citrate}} = N_{\text{Octanediol}} = 2 \times 10^{-11}\left(\text{mol cm}^{-2}\text{s}^{-1}\right)$$

Since the molar flux into bone tissue volume should be equal to that out of the bone tissue volume (Eq. (1.9)), the concentration C_R on the implant surface (r = R) could be determined:

$$C_{\text{Citrate}} = C_{\text{Octanediol}} = 2.2 \times 10^{-10}\left(\text{mol cm}^{-3}\right)$$
$$= 2.2 \times 10^{-4}\left(\text{mmol L}^{-1}\right)$$

3. Results

3.1. Cytotoxicity evaluation of 1,8-Octanediol and Citrate

To evaluate the cytotoxicity of 1,8-Octanediol and Citrate, 1,8-Octanediol solution was freshly prepared before each study and pH adjusted Citrate solution was used in the present study to rule out the pH effect, while SDS producing consistent positive cytotoxicity to cells according to the ISO 10993-5:20019(E) was selected as a positive control. Given 3T3 mouse fibroblast is an established cell line widely used for cytotoxicity evaluation, we first studied the cytotoxicity of 1,8-Octanediol and Citrate to 3T3 cells. Within the nontoxic concentration range, the cytotoxicity seemed to be comparable while Citrate induced less cytotoxicity compared with 1,8-Octanediol at high, toxic concentrations (Fig. 2A), given reduction of cell viability by less than 30% is considered a noncytotoxic effect according to ISO 10993-5:2009(E). Meanwhile, SDS at concentrations as low as 0.2 mg/mL showed 99% reduction of cell viability, demonstrating an appropriate test system response. Further, cytotoxicity towards MG63, an established human osteosarcoma-derived cell line commonly used as osteoblastic models in orthopedic studies, showed a comparable concentration-response curve between Citrate and 1,8-Octanediol treatment; however, Citrate seemed to induce less reduction in cell viability at nontoxic concentrations (Fig. 2B). Next, primary human bone marrow derived
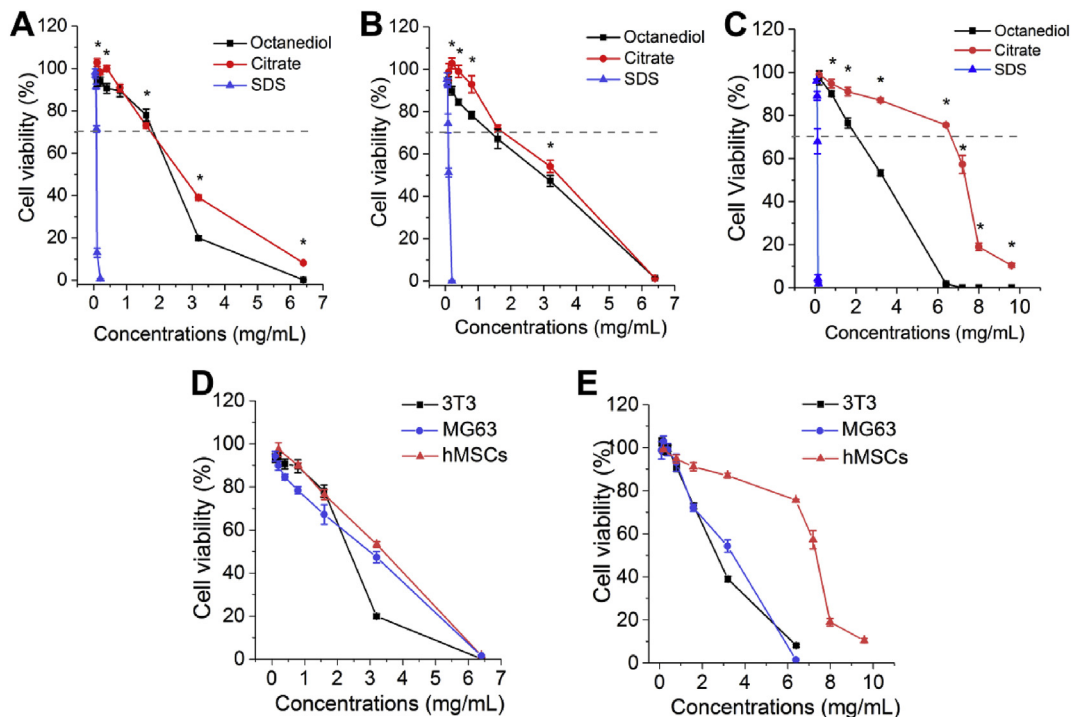

Fig. 2. Cytotoxicity evaluation of 1,8-Octanediol and Citrate.(A) Cytotoxicity of 1,8-Octanediol, Citrate and SDS as positive control to 3T3, (**B**) MG63, and (**C**) hMSCs (* indicating P < 0.05). (**D**) Cell-specific cytotoxicity of 1,8-Octanediol and (**E**) Citrate to different cells.
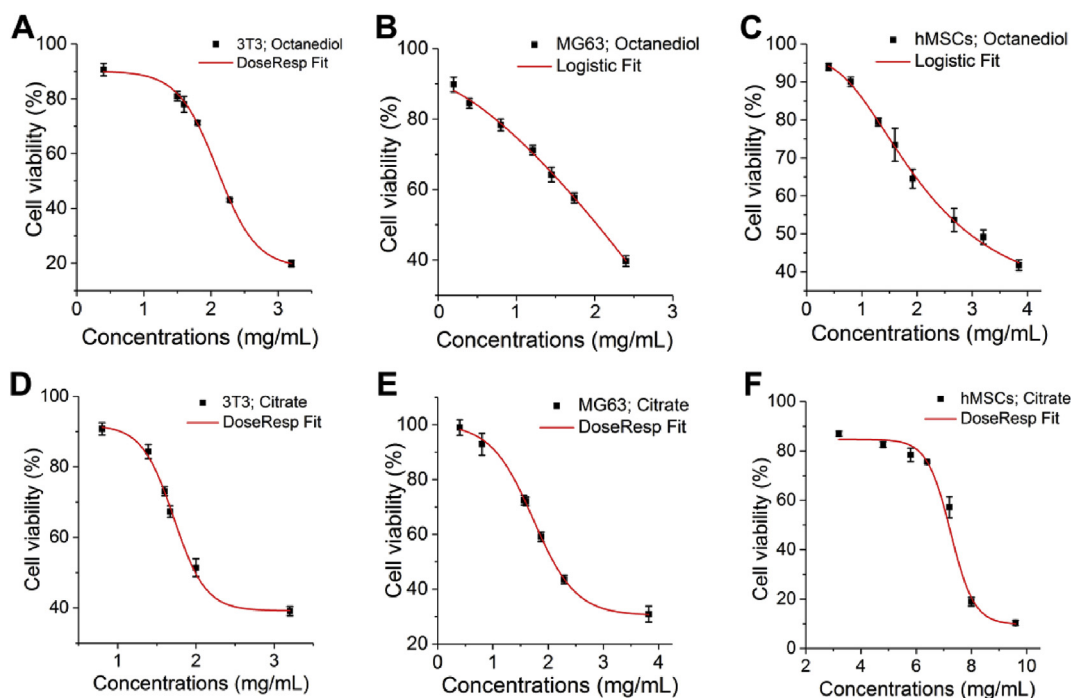
Fig. 3. Fitted curves for the viability-concentration response. (**A**) DoseResp Fit of the viability-concentration response of 3T3 to Octanediol. (**B**) Logistic Fit of the viability-concentration response of MG63 to Octanediol. (**C**) Logistic Fit of the viability-concentration response of hMSCs to Octanediol. (**D**) DoseResp Fit of the viability-concentration response of 3T3 to Citrate. (**E**) DoseResp Fit of the viability-concentration response of MG63 to Citrate. (**F**) DoseResp Fit of the viability-concentration response of hMSCs to Citrate.

mesenchymal stem cells (hMSCs), responsible for bone formation after osteogenic differentiation, were studied and a surprisingly high tolerance of hMSCs to Citrate was found. Citrate induced a much more reduced cytotoxic effect compared to 1,8-Octanediol (Fig. 2C). By comparing the same monomer to different cells, it was clear that there was a cell-specific response to the monomers. 1,8-Octanediol induced a similar concentration-viability response profile to both bone related MG63 and hMSCs, which was different from the profile to 3T3 (Fig. 2D). On the other hand, the concentration-viability response profile of both 3T3 and MG63 in response to Citrate was similar, while hMSCs again showed a surprisingly high tolerance to Citrate (Fig. 2E).

To estimate the critical concentration of both 1,8-Octanediol and Citrate to induce cytotoxicity: that is, the concentration resulting in less than 30% reduction in cell viability, also called EC30, as well as the widely investigated effective concentration EC50, at least 6 different concentrations of both Citrate and 1,8-Octanediol that could induce a reduction of cell viability within the range from 10% to 90% were selected for the preparation of a fitted curve of the concentration-viability response as shown in Fig. 3. Curves representing the 1,8-Octanediol effect to MG63 (Fig. 3B) and hMSCs (Fig. 3C) were fit with Logistic, while all the other curves could be fit with DoseResp. Based on the fitted curves, EC30 and EC50 of both 1,8-Octanediol and Citrate in molar concentrations to different cells was listed in Table 1 to better compare the cytotoxicity, since POC synthesis was largely performed at 1:1 M feeding ratio of the two monomers. EC30 and EC50 of monomers in mg/mL, which could be translated to weight measurement in *in vivo* studies such as mg/Kg, was also provided in Table 1 [30]. Basically, a higher EC30 value suggests a wider range of noncytotoxic concentrations. Compared with Citrate, 1,8-Octanediol surprisingly seemed to have a higher EC30 value and a comparable EC30 value when incubating with 3T3 and MG63 permanent cell lines, respectively, suggesting that to 3T3, 1,8-Octanediol possessed a wider range of noncytotoxic concentrations compared to Citrate. In comparison, Citrate presented a

markedly wider range of nontoxic concentrations on primary hMSCs, the EC30 of which was ~4 times higher than that of 1,8-Octanediol. Moreover, by analyzing the important and most investigated parameter EC50 (the concentration where cell viability was inhibited by 50%) (Table 1), a consistent trend was found: 1,8-Octanediol was less cytotoxic than Citrate to both 3T3 and MG 63 cells, while hMSCs consistently showed a high tolerance to Citrate.

3.2. Immune evaluation of citrate and 1,8-Octanediol

Monocytes are among the first batch of cells to get in contact with implanted biomaterials and play a critical role in the biological response to biomaterials by mediating much of the inflammatory response [31]. Therefore, it is of great importance to evaluate the biocompatibility of materials through evaluating the triggered immune responses to materials [26,32] as well as components of the materials [33]. THP-1 model monocyte cell line was selected in the present study to test the biocompatibility of 1,8-Octanediol and Citrate through the quantification of pro-inflammatory factor expression, since THP-1 cells have been found to respond equivalently to human native peripheral blood monocytes (PBM) in contact with biomaterials, particularly orthopedic implants [34]. As a result, compared with the positive group using 50 ng of LPS for activation, the production of pro-inflammatory tumor necrosis factor-α (TNF-α) in both 1,8-Octanediol and Citrate treatment groups was markedly lower, and no significant difference was observed between 1,8-Octanediol and Citrate groups at different concentrations (Fig. 4A). Meanwhile, 1,8-Octanediol was found to induce more IL-1β production compared to Citrate, but the released IL-1β amount was still substantially lower than that in the LPS positive group (Fig. 4B) and was also much lower than the reported IL-1β concentration in human serum (normal range: 0–5 pg/mL) [35], indicating that both Citrate and 1,8-Octanediol at tested concentrations also did not substantially stimulate the release of IL-1β

Table 1
EC30 and EC50 value (mmol/L or mg/mL) of 1,8-Octanediol and Citrate to different cells.

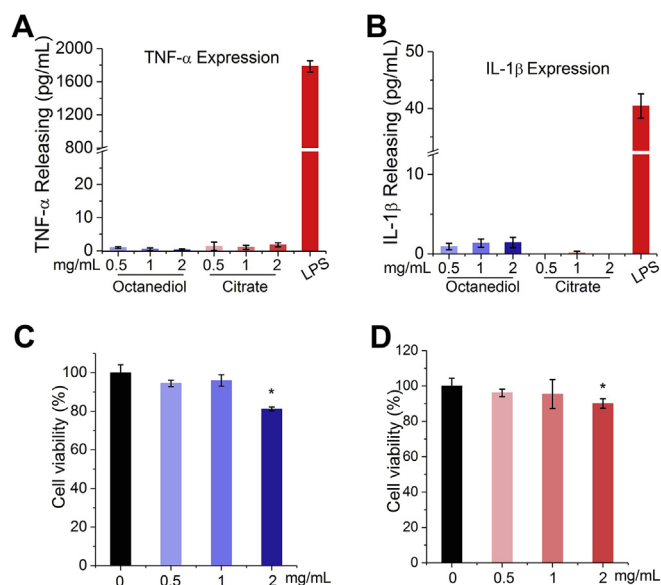| Monomer	EC30 mmol/L (or mg/mL)			EC50 mmol/L (or mg/mL)		
	3T3	MG63	hMSCs	3T3	MG63	hMSCs
1,8-Octanediol	12.5 (or 1.8)	8.4 (or 1.2)	11.8 (or 1.7)	14.8 (or 2.2)	13.8 (or 2.0)	20.2 (or 3.0)
Citrate	8.6 (or 1.7)	8.5 (or 1.6)	34.5 (or 6.6)	10.5 (or 2.0)	10.9 (or 2.1)	37.3 (or 7.2)

Fig. 4. Immune evaluation of the biocompatibility of 1,8-Octanediol and Citrate.(**A**) TNF-α production and (**B**) IL-1β production by THP-1 cells incubated with different concentrations of 1,8-Octanediol and Citrate. Cell viability of THP-1 cells incubated with different concentrations of (**C**)1,8-Octanediol and (**D**) Citrate compared with control group with no monomers added (Set to 100%; * indicating P < 0.05).

Fig. 5. Effect of 1,8-Octanediol and Citrate on hMSCs proliferation.(**A**) Effect of 1,8-Octanediol and(**B**) Citrate at different concentrations on the proliferation of hMSCs. Relative proliferation rate of hMSCs with the treatment of (**C**) 1,8-Octanediol and (**D**) Citrate compared with control group with no monomers added (Set to 1; Proliferation rate = increased cell viability/Day).

from monocytes. Moreover, cell viability of THP-1 cells after incubation with Citrate or 1,8-Octanediol was tested, and as shown in Fig. 4C, no significant decrease in cell viability was observed until the concentration of 1,8-Octanediol or Citrate reached 2 mg/mL. Even at this concentration, cell viability was still reduced less than 30%, which can be considered nontoxic, indicating the changes in pro-inflammatory cytokine production stimulated by 1,8-Octanediol and Citrate treatment at different concentrations were not due to the change in cell viability. Taken together, these results suggest that both 1,8-Octanediol and Citrate at the tested concentrations did not trigger undesired immune response and are compatible with the monocytes.

3.3. Effect of citrate and 1,8-Octanediol on hMSCs proliferation

Bone formation is a complex process involving the differentiation of hMSCs into bone forming osteoblasts, which is essentially controlled by the number and activity of bone forming cells [36]. Therefore, next to viability, the effect of Citrate and 1,8-Octanediol within the nontoxic concentration range on hMSC cell growth was studied by measuring the overall metabolic activity using CCK-8. In the absence of any additional chemical, an almost linear proliferation profile of hMSCs can be observed from day 1 to day 5 (Fig. 5A). By adding 1,8-Octanediol at concentrations of 0.1 mg/mL, an immediate decrease of cell viability can be seen at day 1, and a gradual decrease in proliferation rate from day 1 to day 3 was shown in Fig. 5C with increased 1,8-Octanediol concentration. However, the proliferation rate of hMSCs at day 3-day 5 in groups with 1,8-
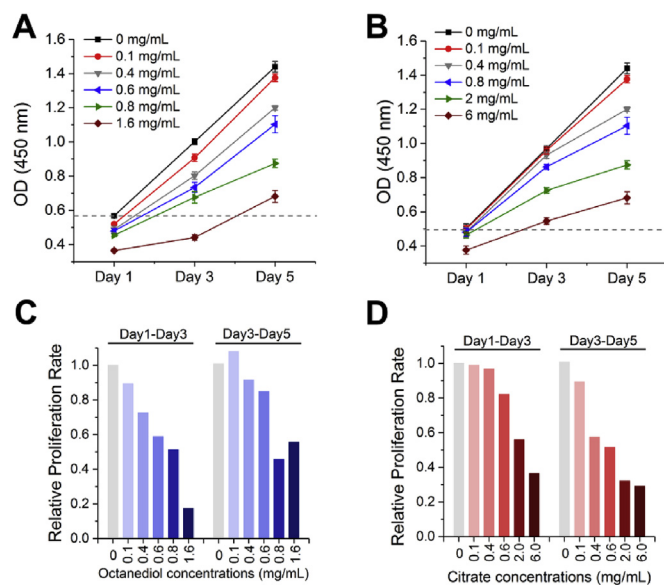
Octanediol at concentrations of ≤0.6 mg/mL was found to further increase compared with that at day 1-day 3, probably because at these concentrations the immediate inhibitory effect from 1,8-Octanediolmay not last long, allowing cells to recover from the reduced cell viability and then display robust cell proliferation during day 3-day 5. Also, although 1,8-Octanediol at 1.6 mg/mL greatly decreased the proliferation rate over the first 3 days, the increased proliferation rate at day 3-day 5 together with a higher cell viability value at day 5 compared to the control group at day 1 (dashed line in Fig. 5A) indicated that the hMSCs in the group still retained their proliferation potential although their growth capability was greatly inhibited by 1.6 mg/mL of 1,8-Octanediol.

In contrast, after 1 day of incubation, Citrate supplementation only reduced cell viability significantly when its concentration reached as high as 6 mg/mL (Fig. 5B), and the proliferation rate at day 1-day 3 started to decrease only after its concentration increased to 0.8 mg/mL (Fig. 5D). Moreover, Citrate treatment was shown to have a relatively slower effect on cell growth compared with 1,8-Octanediol treatment, presented as a gradually decreased proliferation rate, especially at day 3-day 5, with increased Citrate concentration. Interestingly, cells retained their ability to proliferate with Citrate treatment even at concentrations of 6 mg/mL, which further supported our previous finding that hMSCs have a surprisingly high tolerance to extracellular Citrate. Taken together, 1,8-Octanediol was found to have an immediate effect on cell proliferation while Citrate has a relatively slower effect, and compared with 1,8-Octanediol, Citrate showed less inhibitory effect on hMSCs proliferation.

3.4. Effect of citrate and 1,8-Octanediol on osteogenic differentiation

The next level of *in vitro* biocompatibility evaluation is to test the effect of the two monomers on the specific functionalities of hMSCs. The production of functional proteins such as alkaline phosphatase (ALP), reflecting the activity of bone forming cells, is a vital part of biocompatibility evaluation *in vitro*. Therefore, we further studied the effect of Citrate and 1,8-Octanediol on the production of ALP, the enzyme critical for the subsequent biomineralization process and regarded as the middle stage osteogenic marker [37], after differentiation was initiated by well-established osteogenic medium. As shown in Fig. 6A, after differentiation for 14 days, 1,8-Octanediol at 0.4 mg/mL in osteogenic medium started to decrease the ALP production. 0.6 mg/mL of 1,8-Octanediol decreased ALP production almost 50% compared with the control group and significantly decreased the DNA production (Fig. 6B), indicating 0.6 mg/mL of 1,8-Octanediol not only decreased the osteoblast number but also their bone forming activity. In contrast, Citrate had no significant effect on both ALP activity and total DNA amount at all concentrations tested, indicating a better functional biocompatibility of Citrate compared with 1,8-Octanediol for hMSCs undergoing osteogenic differentiation. From the ALP staining results (Fig. 6C), it was obvious that with increased 1,8-Octanediol concentration, the positive staining for ALP in differentiating hMSCs was reduced but still higher than that in undifferentiated hMSCs cultured in growth medium, where nearly no positive staining of ALP could be observed, indicating the hMSCs exposed to 0.6 mg/mL of 1,8-Octanediol still retained their functionality.

4. Discussion

Biodegradable poly(octamethylene citrate) (POC)/HA composites have shown impressive performance in orthopedic applications in terms of eliciting minimal inflammatory response and robust peri-implant bone formation [5,8,10]. However, surprisingly limited information is available about the cytocompatibility of the

Fig. 6. Effect of 1,8-Octanediol and Citrate on hMSCs differentiation. (**A**) Relative ALP activity, (**B**) Total DNA amount, and (**C**) ALP staining of hMSCs differentiated in osteogenic medium with 1,8-Octanediol or Citrate supplemented after 14 days compared with control group with no monomers added (Set to 100%; * indicating P < 0.05).

two monomers for POC synthesis. Therefore, in the present study, the cytobiocompatibility of both 1,8-Octanediol and Citrate in orthopedic applications was investigated in terms of acute cytotoxicity, immune response and long-term functionality evaluation. We chose to investigate Citrate instead of Citric Acid because it allows us to compare the cytobiocompatibility of the two chemicals excluding the interference of pH change, since POC degrades via surface erosion [5] and is composited with HA for orthopedic applications, limiting the release of acidic byproducts versus bulk degradation and providing some pH buffering due to the presence of HA.

Determination of cell viability is an established measurement endpoint recommended by the ISO standard for *in vitro* basal cytotoxicity assessment [30], which is very important in determining the cytocompatibility of the two monomers. Based on cytotoxicity assay, the critical tolerant concentration representing the concentration inhibiting 30% of cell viability (EC30) which provides the nontoxic concentration range, as well as the EC50 estimations which could assist the prediction of the starting dose for *in vivo* acute lethality assays can be determined [30]. Based on both EC30 and EC50, it has been found that to both 3T3 and MG63 cells, 1,8-Octanediol surprisingly seemed to be equivalently or even less cytotoxic than Citrate. In fact, 3T3 is a well-established cell line probably most frequently used for cytotoxicity evaluation of various chemicals, which allows us to compare the cytotoxicity of the two monomers with other chemicals. For example, the EC50 value of both Citrate and 1,8-Octanediol to 3T3 was much higher than that of all the resin monomers and initiators tested previously [24], and even higher than that of ascorbic acid (EC50: 0.49 mg/mL), the vitamin C we orally supplement [30], indicating the low cytotoxicity of 1,8-Octanediol and Citrate. Additionally, immune evaluation results show that no undesired pro-inflammatory response is triggered by either monomer. Interestingly, with regard to hMSCs, both EC30 and EC50 data revealed an unusually high tolerance of hMSCs to Citrate but not to 1,8-Octanediol, probably because hMSCs, as a type of multipotent cell, has a distinct metabolic pattern from the two specialized cells, 3T3 and MG63, and hMSCs may have the capability of somehow consuming extracellular Citrate as an energy-rich metabolite. In fact, metabolism of extracellular Citrate has been found previously in neuron cells [38,39] and metastatic cancer cells [40,41]. Whether hMSCs could consume Citrate remains unknown; however, it is highly worthy of further exploration. In the functionality evaluation, Citrate after long-term incubation with hMSCs also showed less inhibitory effect on both cell proliferation and differentiation compared with 1,8-Octanediol at the same concentrations, suggesting during degradation, accumulation of 1,8-Octanediol tends to affect bone formation earlier.

One has to note that the major drawback of these *in vitro* cytobiocompatibility tests is the difficulty of assessing the relevance of the obtained results to the *in vivo* situation. Other than the established RC (Registry of Cytotoxicity) prediction model [30] that would help determine the starting dose for *in vivo* acute toxicity study from *in vitro* cytotoxicity results, it would also be helpful to estimate the *in vivo* situation based on the degradation mode of the polymer and the diffusion of the monomers in bone. To that end, we established a model of monomer diffusion from a cylindrical POC/HA implant in bone. Bone is considered as porous media with complex microgeometry [42] and bone is also highly vascularized to deliver oxygen and nutrients to tissues and remove metabolic wastes [43]. More importantly, to supply all cells with sufficient nutrients in native tissue, all cells have to be within 200 μm from a blood vessel [27]. Together with the fact that the vasculature in bone is mostly very delicate with very thin walls [44], the time for the monomers to flux into the blood stream through vessel walls
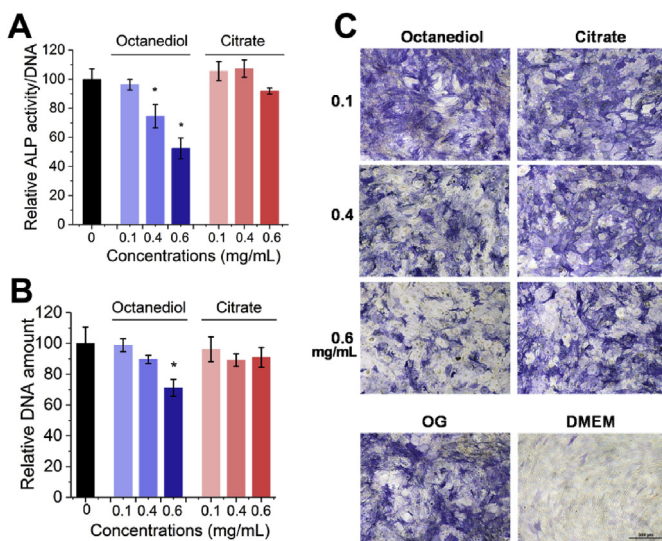
compared with the time to diffuse toward the blood vessels is short enough for the monomer concentrations at the outer surface of blood vessels to be 0. If we then simplify our model by assuming the transport is only in the radial direction, after the cylindrical POC/HA composite is implanted, there is a concentration gradient of released monomers between our implant surface (concentration set to C_R) and the blood vessel rich surface where the monomer concentration C_{R1} is 0, with the annular cylinder space between the two surfaces representing bone tissue that could be affected by degradation products as shown in Fig. 1. In this way, we could consider only one-dimensional radial diffusion (Fig. 1) and the molar flux of monomers transported from the bone tissue volume into blood (Eq. (1.9)) could be estimated based on the radial diffusion model in cylindrical coordinates [28]. The detailed solution for the diffusion problem can be found in **Materials and Methods 2.9**.

POC degrades through surface erosion [5], and the polymer degradation rate is directly proportional to the surface area. The degradation of POC/60%HA(2.7 mm(D) × 4 mm (L)) lasted for at least 1 year *in vivo* [8], a sufficiently large time scale compared with the cytotoxicity and even the functionality experiment conducted in the present study to justify the assumption that the implant surface area within the time of investigation remains unchanged, allowing us to consider the surface erosion as zero order release., suggesting the release rate of monomers is constant. Therefore, for POC/60%HA implants introduced above with the estimated weight of 140 mg (Eq. (2.1)), the total molar mass of Citrate and 1,8-Octanediol in the implant 0.165 mmol. Assuming the implant could degrade completely in 1 year, the molar flux of monomers into the bone tissue can be calculated according to Eq. (2.2) and more importantly, the molar flux into and out of the bone tissue volume (Eq. (1.9)) should be equal, which eventually leads us to estimate the C_R value at the implant surface of 2.2×10^{-4} mmol/L for both Citrate and 1,8-Octanediol. These values represent the maximum concentration of monomers in contact with bone tissue, lower than the critical cytotoxic concentrations (Table 1) as well as the 1,8-Octanediol concentration (0.4 mg/mL or 2.7 mmol/L) affecting hMSCs differentiation obtained in the present *in vitro* study, indicating the cytocompatibility of these two monomers during degradation in orthopedic settings. Of note, the diffusion coefficient D (0.0198 mm^2/min) in mice cortical bone we used in Eq. (1.8) was derived from sodium fluorescein (MW:~400 Da) [29], the molecular weight of which is higher than both Octanediol and Citrate, suggesting more rapid diffusion of either monomer than fluorescein. Also, the above model could also be very helpful to estimate the C_R value at the implant surface of other cylindrical citrate-based materials with different sizes in orthopedic applications. One must still note that the model is based on ideal situations and assumptions. Thus it would still be important to evaluate the compatibility of monomers in future *in vivo* studies.

In conclusion, the above work has studied the cytobiocompatibility of 1,8-Octanediol and Citrate *in vitro* in terms of acute cytotoxicity, immune response, and long-term functionality evaluation for the first time. In comparison, 1,8-Octanediol was found to have less acute toxicity to 3T3 fibroblasts than Citrate while presenting comparable cytotoxicity to MG63 osteoblast-like cells. However, Citrate has shown impressively increased compatibility with hMSCs compared to 1,8-Octanediol. Minimal immune response was observed for both Citrate and Octanediol. The critical cytotoxic concentrations and the critical concentrations for hMSCs to maintain their functionality unaffected are provided, together with the diffusion model of released Citrate and 1,8-Octanediol during degradation. The cytocompatibility of these two monomers in citrate-based composites during degradation in an orthopedic setting was demonstrated, and the obtained model would also

provide guidance for the estimation of other cylindrical citrate-based orthopedic materials with different sizes. Taken as a whole, the present study has demonstrated the excellent biocompatibility of the monomer components of POC and provides strong encouragement for the successful application of POC composites as a new class of orthopedic biomaterials *in vivo*.

Conflicts of interest

Dr. Yang and The Pennsylvania State University have a financial interest in Aleo BME, Inc. and Acuitive Technologies, Inc. These interests have been reviewed by the University's Institutional and Individual Conflict of Interest Committees and are currently being managed by the University.

Acknowledgements

References

[1] P.P. Spicer, et al., Evaluation of bone regeneration using the rat critical size calvarial defect, Nat. Protoc. 7 (10) (2012) 1918–1929.

[2] J.A. Hunt, J.T. Callaghan, Polymer-hydroxyapatite composite versus polymer interference screws in anterior cruciate ligament reconstruction in a large animal model, Knee Surg. Sports Traumatol. Arthrosc. 16 (7) (2008) 655–660.

[3] R.J. Kane, G.L. Converse, R.K. Roeder, Effects of the reinforcement morphology on the fatigue properties of hydroxyapatite reinforced polymers, J. Mech. Behav. Biomed. Mater. 1 (3) (2008) 261–268.

[4] A.J. Wagoner Johnson, B.A. Herschler, A review of the mechanical behavior of CaP and CaP/polymer composites for applications in bone replacement and repair, Acta Biomater. 7 (1) (2011) 16–30.

[5] R.T. Tran, J. Yang, G.A. Ameer, Citrate-based biomaterials and their applications in regenerative engineering, Annu. Rev. Mater. Res. 45 (2015) 277–310.

[6] K.E. Uhrich, et al., Polymeric systems for controlled drug release, Chem. Rev. 99 (11) (1999) 3181–3198.

[7] Y. Guo, et al., Citrate-based biphasic scaffolds for the repair of large segmental bone defects, J. Biomed. Mater. Res. A 103 (2) (2015) 772–781.

[8] E.J. Chung, et al., Long-term in vivo response to citric acid-based nanocomposites for orthopaedic tissue engineering, J. Mater. Sci. Mater. Med. 22 (9) (2011) 2131–2138.

[9] J. Yang, A.R. Webb, G.A. Ameer, Novel citric acid-based biodegradable elastomers for tissue engineering, Adv. Mater. 16 (6) (2004), p. 511–+.

[10] J. Yang, et al., Synthesis and evaluation of poly(diol citrate) biodegradable elastomers, Biomaterials 27 (9) (2006) 1889–1898.

[11] J.P. Kim, et al., Citrate-based fluorescent materials for low-cost chloride sensing in the diagnosis of cystic fibrosis, Chem. Sci. 8 (1) (2017) 550–558.

[12] Y. Su, et al., Design strategies and applications of circulating cell-mediated drug delivery systems, ACS Biomater. Sci. Eng. 1 (4) (2015) 201–217.

[13] A.S. Wadajkar, et al., Dual-imaging enabled cancer-targeting nanoparticles, Adv. Healthc Mater. 1 (4) (2012) 450–456.

[14] J. Guo, et al., Click chemistry plays a dual role in biodegradable polymer design, Adv. Mater. 26 (12) (2014) 1906–1911.

[15] Y. Zhang, et al., Fluorescence imaging enabled urethane-doped citrate-based biodegradable elastomers, Biomaterials 34 (16) (2013) 4048–4056.

[16] J. Dey, et al., Crosslinked urethane doped polyester biphasic scaffolds: potential for in vivo vascular tissue engineering, J. Biomed. Mater. Res. A 95 (2) (2010) 361–370.

[17] Z. Xie, et al., Development of intrinsically photoluminescent and photostable polylactones, Adv. Mater. 26 (26) (2014) 4491–4496.

[18] J. Yang, et al., Development of aliphatic biodegradable photoluminescent polymers, Proc. Natl. Acad. Sci. U S A 106 (25) (2009) 10086–10091.

[19] D. Shan, et al., Flexible biodegradable citrate-based polymeric step-index optical fiber, Biomaterials 143 (2017) 142–148.

[20] Z. Xie, et al., Immune cell-mediated biodegradable theranostic nanoparticles for melanoma targeting and drug delivery, Small 13 (10) (2017).

[21] S. Kalaba, et al., Design strategies and applications of biomaterials and devices for Hernia repair, Bioactive Mater. 1 (1) (2016) 2–17.

[22] Y. He, W. Wang, J. Ding, Effects of L-lactic acid and D,L-lactic acid on viability and osteogenic differentiation of mesenchymal stem cells, Chin. Sci. Bull. 58 (20) (2013) 2404–2411.

[23] K. Moharamzadeh, et al., Cytotoxicity of resin monomers on human gingival fibroblasts and HaCaT keratinocytes, Dent. Mater. 23 (1) (2007) 40–44.

[24] W. Geurtsen, et al., Cytotoxicity of 35 dental resin composite monomers/additives in permanent 3T3 and three human primary fibroblast cultures, J. Biomed. Mater. Res. 41 (3) (1998) 474–480.

[25] M. Pommet, et al., Intrinsic influence of various plasticizers on functional properties and reactivity of wheat gluten thermoplastic materials, J. Cereal.

Sci. 42 (1) (2005) 81–91.

[26] D. Motlagh, et al., Hernocompatibility evaluation of poly(glycerol-sebacate) in vitro for vascular tissue engineering, Biomaterials 27 (24) (2006) 4315–4324.

[27] J. Rouwkema, A. Khademhosseini, Vascularization and angiogenesis in tissue engineering: beyond creating static networks, Trends Biotechnol. 34 (9) (2016) 733–745.

[28] G.A. Truskey, F. Yuan, D.F. Katz, Transport Phenomena in Biological Systems, 2004.

[29] L. Wang, et al., In situ measurement of solute transport in the bone lacunar-canalicular system, Proc. Natl. Acad. Sci. U S A 102 (33) (2005) 11911–11916.

[30] ICCVAM, Guidance Document on Using in Vitro Data to Estimate in Vivo Starting Doses for Acute Toxicity, 2001. NIH Publication No. 01–4500.

[31] J.E. Davies, Understanding peri-implant endosseous healing, J. Dent. Educ. 67 (8) (2003) 932–949.

[32] T. Ding, J. Sun, P. Zhang, Immune evaluation of biomaterials in TNF-alpha and IL-1beta at mRNA level, J. Mater. Sci. Mater. Med. 18 (11) (2007) 2233–2236.

[33] T. Heil, et al., Human peripheral blood monocytes versus THP-1 monocytes for in vitro biocompatibility testing of dental material components, J. Oral Rehabil. 29 (5) (2002) 401–407.

[34] S.H. Lee, et al., Human monocyte/macrophage response to cobalt-chromium corrosion products and titanium particles in patients with total joint replacements, J. Orthop. Res. 15 (1) (1997) 40–49.

[35] M. Alecu, et al., The interleukin-1, interleukin-2, interleukin-6 and tumour necrosis factor alpha serological levels in localised and systemic sclerosis, Rom. J. Intern. Med.Revue roumaine de medecine interne 36 (3–4) (1998) 251–259.

[36] U. Kini, B.N. Nandeesh, Physiology of Bone Formation, Remodeling, and Metabolism, 2012, pp. 29–57.

[37] C. Zhang, et al., Inhibition of Wnt signaling by the osteoblast-specific transcription factor Osterix, Proc. Natl. Acad. Sci. U S A 105 (19) (2008) 6936–6941.

[38] M.E. Mycielska, et al., Extracellular citrate in health and disease, Curr. Mol. Med. 15 (10) (2015) 884–891.

[39] G.R. Stoppa, et al., Intracerebroventricular injection of citrate inhibits hypothalamic AMPK and modulates feeding behavior and peripheral insulin signaling, J. Endocrinol. 198 (1) (2008) 157–168.

[40] M.E. Mycielska, et al., Citrate enhances in vitro metastatic behaviours of PC-3M human prostate cancer cells: status of endogenous citrate and dependence on aconitase and fatty acid synthase, Int. J. Biochem. Cell Biol. 38 (10) (2006) 1766–1777.

[41] Y. Hua, et al., Dynamic metabolic transformation in tumor invasion and metastasis in mice with LM-8 osteosarcoma cell transplantation, J. Proteome Res. 10 (8) (2011) 3513–3521.

[42] G.H. Goldsztein, Transport of nutrients in bones, SIAM J. Appl. Math. 65 (6) (2005) 2128–2140.

[43] M. Marenzana, T.R. Arnett, The key role of the blood supply to bone, Bone Res. 1 (3) (2013) 203–215.

[44] B. Roche, et al., Structure and quantification of microvascularisation within mouse long bones: what and how should we measure? Bone 50 (1) (2012) 390–399.